Advanced Filter Design Using Cross-Coupled Networks With Higher-Order Resonances

Marjan Mokhtaari[1], Jens Bornemann[1] and Smain Amari[2]

[1] University of Victoria, Victoria, BC, Canada V8W 3P6
[2] Royal Military College of Canada, Kingston, ON, Canada K7K 7B4

***Abstract* — A new class of cross-coupled networks is presented for the advanced design of microwave filters. By including nodes for higher/lower-order mode resonances, a broadband model is obtained which partly eliminates the narrowband restrictions found in current coupling matrix approaches. Several bandpass filter examples for WR75 waveguide applications are presented. It is demonstrated that the new cross-coupled network correctly predicts all resonance effects over a wide frequency range. The process is validated by comparison with in-house and commercially available field-theory-based codes.**

I. Introduction

Microwave and millimeter-wave bandpass filters play an important role in modern communication systems since the allocation of frequency bands corresponding to different usages or services imposes strict filter requirements. Sharp cutoff skirts, low in-band insertion loss and asymmetric frequency responses can be created by cross-coupled or bypassed resonator arrangements which produce transmission zeros at finite frequencies.

A general theory of coupled resonator bandpass filters was presented in the 1970s [1] and is still widely used. A slightly different approach [2, 3] determines the filtering function for specified locations of transmission zeroes. Recent activities focused on the optimization [4] and synthesis [5] of networks including source-load coupling. Moreover, the concept of non-resonating nodes was introduced [6].

All filter design approaches utilizing cross-coupled networks are valid only in the vicinity of the filter passband. This is due to the fact that only those electric resonances are considered which describe the filter performance over an acceptable bandwidth. However, higher-order mode resonances in waveguide filters can be advantageously utilized to create additional transmission zeros and/or filter passbands. It is thus of fundamental importance that such effects, which have a profound influence on the final filter performance, be included from the onset of a filter design procedure.

Therefore, in this paper, we present a new configuration of the cross-coupled network, which accounts for higher-order mode resonances through a framework of resonating nodes. It is demonstrated that the performances predicted from this model's coupling matrices agree over a wide frequency range with results of full-wave electromagnetic codes.

II. Theoretical Approach and Network Model

The basic concept of a cross-coupled network composed of N coupled lossless resonators and its governing equations are discussed in [4] and will not be repeated here. In order to improve the flexibility of this network, we are adding provisions for non-resonating nodes according to [6].

Within this framework, each actual cavity is modeled by its main resonance, which is associated with the filter passband, and by one or more higher-order resonances, which are viewed as being completely detuned. As an example, consider the coupling scheme shown in Fig. 1.

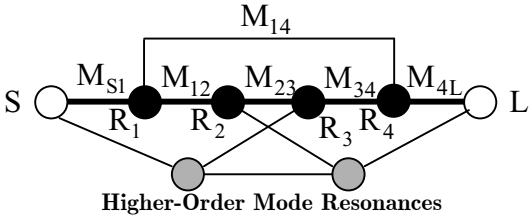

Fig. 1. A possible coupling scheme of a quadruplet with two higher-order mode resonances.

The dark inline resonances together with the source and load nodes represent the filter behaviour in the vicinity of the passband. Since the gray higher-order nodes are tuned to higher-order mode resonances, their influence on the filter passband is minimal. At their respective resonance frequencies, however, they dominate and might even use a path through the inline nodes of Fig. 1 as bypass coupling to create transmission zeros. Their connection to source, load or other nodes is determined by a comparison between the responses of the actual filter, i.e. using a field solver, and the coupling matrix. It will be shown that in order to meet the frequencies of some additional higher-order effects, only a certain connection of the higher-order nodes is permitted.

In order to apply this technique to the broadband design of filters, the additional passbands or transmission zeros attributed to higher-order mode resonances can be specified beforehand. The coupling matrix can then be obtained by optimization, keeping in mind that the coupling coefficient values for non-resonating nodes are constant and do not contribute a frequency term. In this work, the optimization of the coupling matrix is carried

out using the Gauss Newton Algorithm on the error function

$$F = \sum_{i=1}^{N_s}\left(\left|\frac{1}{GIL(f_i)}\right| - \left|\frac{1}{IL(f_i)}\right|\right)^2 + \sum_{i=1}^{N_p}\left(\left|\frac{1}{GRL(f_i)}\right| - \left|\frac{1}{RL(f_i)}\right|\right)^2 + \sum_{i=1}^{N_h}\left(\left|\frac{1}{GIL(f_i)}\right| - \left|\frac{1}{IL(f_i)}\right|\right)^2 + \sum_{i=1}^{N_c}\left(\left|\frac{1}{GRL(f_i)}\right| - \left|\frac{1}{RL(f_i)}\right|\right)^2 \quad (1)$$

where N_s, N_p, N_h and N_c are the number of frequency samples in the stopband, passband, higher-order modes and cutoff frequency regions, respectively; GIL and GRL are the goal values for the insertion loss and return loss, and IL and RL are the actual values during optimization.

III. RESULTS

In this section, we show how higher-order resonances and their correct representation within the coupling matrix aid in the wideband design of filters. The first example is an H-plane folded waveguide tri-section filter as shown in the inset of Fig. 2.

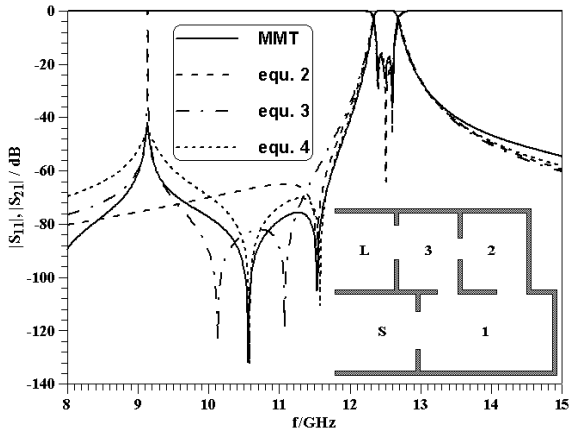

Fig. 2. Performance of folded waveguide tri-section filter; comparison between field-theory analysis and different coupling schemes.

In order to realize the performance with one transmission zero below the passband, the following standard coupling matrix and routing scheme (Fig. 3) was used initially (f_0=12.494GHz, b=0.25GHz):

$$M = \begin{bmatrix} 0.0000 & 1.0408 & 0.0000 & 0.0000 & 0.0000 \\ 1.0408 & -0.0821 & 0.9570 & -0.1150 & 0.0000 \\ 0.0000 & 0.9570 & 0.1022 & 0.9570 & 0.0000 \\ 0.0000 & -0.1150 & 0.9570 & -0.0821 & 1.0408 \\ 0.0000 & 0.0000 & 0.0000 & 1.0408 & 0.0000 \end{bmatrix} \quad (2)$$

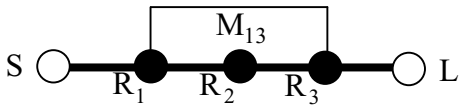

Fig. 3. Routing scheme for equ. (2).

Cavity 1 operates in the TE_{102} mode to produce the correct cross coupling M_{13} (c.f. [7]). Upon realization of the actual filter, however, it was found that two transmission zeros always appear simultaneously (solid lines in Fig.2) and that this behavior is not predicted by the original coupling matrix (dashed lines in Fig. 2). Apparently, the fundamental resonance of the TE_{102} cavity (9.3GHz) creates another path for cross coupling. The first approach to include this behavior in the coupling matrix is shown in (3) and Fig. 4, assuming that a coupling between the two resonances in cavity 1 (the fundamental one being heavily detuned) exists and that a second bypass coupling to resonator 3 is created.

$$M = \begin{bmatrix} 0.0000 & 1.0400 & 0.0000 & 0.0000 & 0.0000 & 0.0000 \\ 1.0400 & -0.0820 & 0.9570 & -0.1150 & -1.0000 & 0.0000 \\ 0.0000 & 0.9570 & 0.1022 & 0.9570 & 0.7500 & 0.0000 \\ 0.0000 & -0.1150 & 0.9570 & -0.0820 & 0.7500 & 1.0400 \\ 0.0000 & -1.0000 & 0.7500 & 0.7500 & 31.750 & 0.0000 \\ 0.0000 & 0.0000 & 0.0000 & 1.0400 & 0.0000 & 0.0000 \end{bmatrix} \quad (3)$$

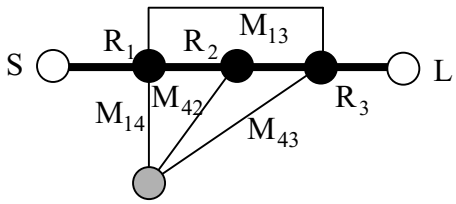

Fig. 4. Routing scheme for equ. (3).

While this approach (dash-dotted line in Fig. 2) captures the fundamental resonance and the two transmission zeros, the values in (3) cannot be adjusted to match their exact positions.

Therefore, the following coupling scheme (Fig. 5 and equ. (4)) is derived. It is based on a simultaneous excitation of the two resonances in cavity 1 through the S-R_1 iris and correctly predicts the locations of the transmission zeros and all resonances (dotted lines in Fig. 2). Note that the original coupling matrix (2) is changed only very slightly by the introduction of the higher-order mode resonance and related paths.

$$M = \begin{bmatrix} 0.0000 & 0.9837 & 0.0000 & 0.0000 & 0.9837 & 0.0000 \\ 0.9837 & -0.0695 & 0.9210 & -0.1280 & 0.0000 & 0.0000 \\ 0.0000 & 0.9210 & 0.1218 & 0.8849 & 0.1350 & 0.0000 \\ 0.0000 & -0.1280 & 0.8849 & -0.0791 & -0.0780 & 1.0301 \\ 0.9837 & 0.0000 & 0.1350 & -0.0780 & 31.8001 & 0.0000 \\ 0.0000 & 0.0000 & 0.0000 & 1.0301 & 0.0000 & 0.0000 \end{bmatrix} \quad (4)$$

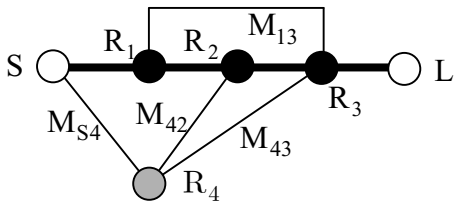

Fig. 5. Routing scheme for equ. (4).

The next example applies to a dual-mode filter commonly known as a quadruplet. This filter was originally presented in [8], and operates with TE_{101} and TE_{011} resonances. Its topology is shown in Fig. 6a. Cross coupling between resonators 1 and 4 in the main path of Fig. 6b provides two transmission zeros, one on each side of the passband. The part of the design, which applies to the current investigation, is the second passband also displaying two transmission zeros (Fig. 6c). Upon studying the higher-order resonances in the two dual-mode cavities, the coupling scheme in Fig. 6b was used

to evaluate the broadband filter performance. Fig. 6c compares the responses of two field-theory-based analyses (CIET and HFSS) with that obtained from the coupling scheme of Fig. 6b. Excellent agreement is observed. The new coupling scheme accurately predicts the second passband due to two higher order-mode resonances and the additional two transmission zeros resulting from the bypass (Fig. 6b), which, since the coupling irises are small, operates in both frequency bands.

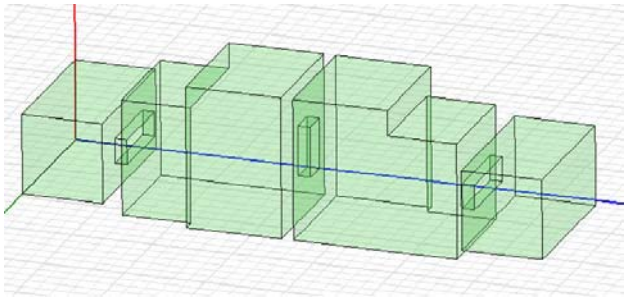

(a)

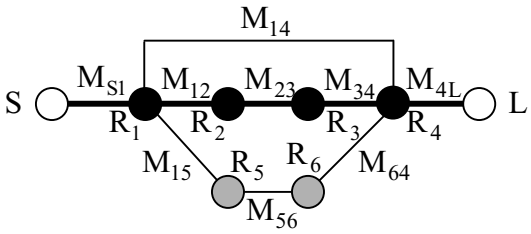

(b)

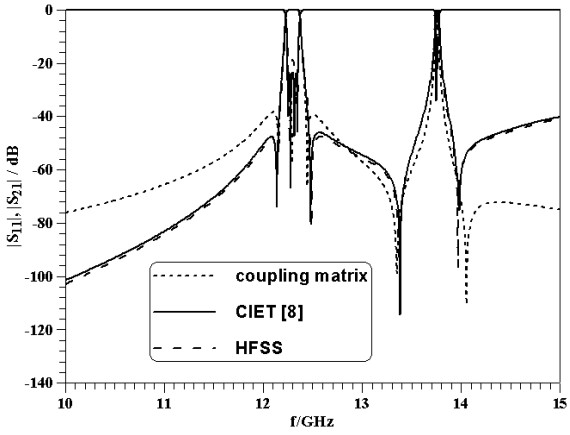

(c)

Fig. 6. Topology and performance of four-pole dual-mode filter (quadruplet); topology (a); coupling scheme (b); comparison between coupling matrix, CIET and HFSS (c).

The final example is a four-pole dual-mode filter based on TE_{101}- and TM_{110}-mode resonances (Fig. 7a). In the main path of the coupling scheme of Fig. 7b, input and output bypass couplings provide two transmission zeros above the passband (Fig. 7c). The second passband at 14.34GHz is created by the next higher-order mode resonances in the two cavities, R_5 and R_6 in Fig. 7b, similar to the concept introduced in the previous example. However and contrary to the behavior of Fig. 6c, a bypass of R_5 and R_6 through the main path is not provided here since the TE_{10}-mode coupling through the center iris is negligible. Thus no transmission zeros are created close to the second passband. In addition to R_5 and R_6, resonances R_7 and R_8 represent the TE_{10}-mode cutoff frequencies in the two cavities. Their influence accounts for the spikes between 10.5 and 10.7 GHz (Fig. 7c). Note that the coupling matrix model of Fig. 7b accounts for all of the resonance effects within a wide bandwidth and that the performance agrees very well with the field-theory-based analyses of the actual filter structure (CIET and HFSS in Fig. 7c).

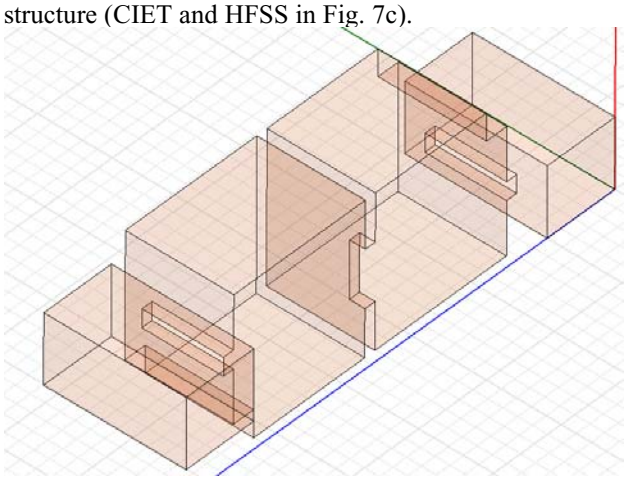

(a)

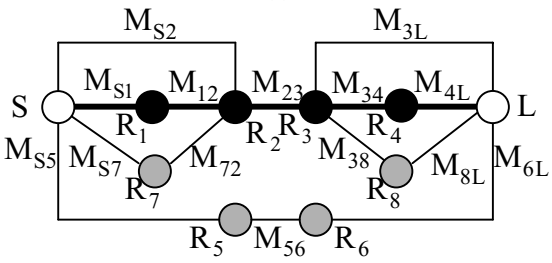

(b)

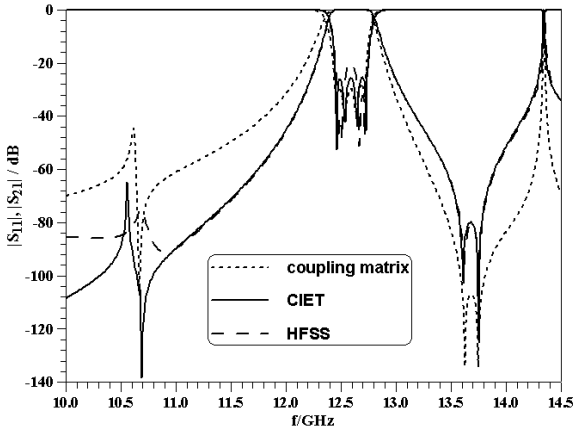

(c)

Fig. 7. Topology and performance of four-pole dual-mode filter with bypass coupling; topology (a); coupling scheme (b); comparison between coupling matrix, CIET and HFSS (c).

Additional resonance effects in this filter occur between 14.5 and 15 GHz (not shown here). Their effects can be included as detuned resonances similar to those of R_5 to R_8 in Fig. 7b.

VI. Conclusion

The concept of coupling matrix filter design is extended to include a wide frequency range. By including nodes for higher/lower-order resonances, the respective waveguide filters can be designed to include these parameters from the start. Consequently, the related effects can be used to improve wideband filter performance and/or create additional characteristics such as, e.g., a second passband. The approach is verified through computation with full-wave codes and commercially available field solvers.

Acknowledgement

The authors wish to thank Uwe Rosenberg of Marconi Communications GmbH, Backnang, Germany for providing the initial filter design of Fig. 7.

References

[1] A.E. Atia and A.E. Williams, "New type of waveguide band pass filters for satellite transponders," *COMSAT Tech. Rev.*, Vol. 1, no. 1, pp. 21-43, 1971.

[2] R.J. Cameron, "Fast generation of Chebychev filter prototypes with a-symmetrically prescribed transmission zeros," *ESA J.*, Vol. 6, pp. 83-95, 1982.

[3] R.J. Cameron, "General prototype network synthesis methods for microwave filters," *ESA J.*, Vol. 6, pp. 193-206, 1982.

[4] S. Amari, U. Rosenberg and J. Bornemann, "Adaptive synthesis and design of resonator filters with source/load-multiresonator coupling," *IEEE Trans. Microwave Theory Tech.*, Vol. 50, pp. 1969-1978, Aug. 2002.

[5] R.J. Cameron, "Advanced coupling matrix synthesis techniques for microwave filters," *IEEE Trans. Microwave Theory Tech.*, Vol. 51, pp. 1-10, Jan. 2003.

[6] S. Amari, U. Rosenberg and J. Bornemann, "Singlets, cascaded singlets, and the non resonating node model for advance modular design of elliptic filter," *IEEE Microwave Wireless Comp..Lett.*, Vol. 14, pp. 237-239, May2004.

[7] R.M. Kurzrok, "General three-resonator filters in waveguide", *IEEE Trans. Microwave Theory Tech.*, Vol. 14, pp. 46-47, Jan. 1966.

[8] J. Bornemann, U. Rosenberg, S. Amari and R. Vahldieck, "Edge-conditioned vector basis functions for the analysis and optimization of rectangular waveguide dual-mode filters", in *1999 IEEE MTT-S Int. Microwave Symp. Dig.*, pp. 1695-1698, Anaheim, USA, June 1999.